KFUPM
Journal of Undergraduate Research International

Diamond Open Access 119

Article Geosciences

Monitoring Carbonate Levels in Saline Water Using Electrical Resistivity in Carbonate Formations

Abdullah Deya Al-Qisoom and Ahmed Al-Yaseri*

Cite https://doi.org/10.64589/juri/221326

Submitted: February 21, 2026 **Revised:** March 17, 2026 **Accepted:** March 25, 2026

ABSTRACT

Geologic carbon capture and sequestration (CCS) is a well-established method for storing large amounts of CO_2. However, monitoring the dissolved carbonate species associated with solubility trapping remains challenging. This study evaluated whether electrical resistivity (ER) can detect the carbonate-rich brines formed during solubility trapping, rather than focusing solely on freephase CO_2. Potassium carbonate (K_2CO_3), a highly conductive tracer, was examined within Austin Chalk limestone cores saturated with solutions ranging from 0.1 to 5 wt% in deionized water (DI) and synthetic produced water (PW). Fluid-only tests showed minimal resistivity variation across a wide range of frequencies (12 Hz–10 kHz), but the resistivity decreased significantly with increasing carbonate concentration. In DI solutions, resistivity dropped from approximately 5.27 Ω· m at 0.1 wt% to 0.16 Ω· m at 5 wt%. When introduced into the Austin Chalk matrix (porosity ~25%–27%), the bulk resistivity increased owing to the resistive nature of the rock, but the inverse relationship between resistivity and carbonate concentration remained consistent. For example, in the K_2CO_2 + PW system at 1 kHz using the 4electrode setup, resistivity decreased from 1.81 Ω· m at 0.1 wt% to 1.50 Ω· m at 5 wt%. Frequency-dependent trends were also observed; higher frequencies (10 kHz) consistently yielded lower resistivities than low-frequency measurements (12 Hz), particularly in rock-saturated systems. Overall, these results establish a quantitative basis for applying electrical geophysical methods to monitor the changes in carbonate concentrations in carbonate reservoirs and support improved longterm CO_2 containment strategies.

Keywords: electrical resistivity, carbonate monitoring, austin chalk, potassium carbonate, produced water, porosity

1. INTRODUCTION

Climate change is a major environmental challenge of the 21st century, with measurable impacts observed across both environmental and engineered systems, including rising land and ocean temperatures, glacier retreat, sea-level rise, and ecosystem degradation [1]. The primary driver of these changes is the accumulation of greenhouse gases (GHGs) in the atmosphere, particularly carbon dioxide (CO_2), which is largely emitted in fossil fuel combustion and industrial activities [2]. Although CO_2 is naturally present and plays an essential role in maintaining Earth's radiative balance, elevated atmospheric concentrations enhance the greenhouse effect and accelerate global warming [3]. Long-term observations indicate that the global mean sea level has risen at an average rate of approximately 1.8 mm/year since 1961, and more than 3 mm/year since the early 1990s, primarily because of thermal expansion and melting of ice masses [4]. Because CO_2 is the dominant GHG emitted by human activities, carbon management technologies are needed along with the use of renewable energy. Hence, the global climate policy focuses on emission reduction, with numerous countries committed to achieve a net-zero target by the mid-century [5]. International climate frameworks, therefore, emphasize deep decarbonization pathways [6].

Among the available mitigation strategies, geological carbon capture and sequestration (CCS) has emerged as a mature and scalable technology capable of reducing emissions from large stationary sources, such as power plants, cement industries, and refineries [2]. In CCS operations, the captured CO_2 is compressed and injected into deep geological formations, including saline aquifers, depleted hydrocarbon reservoirs, and unmineable coal seams [7]. Once injected, CO_2 can be immobilized through multiple trapping mechanisms, including structural, residual, solubility, and long-term mineral trapping [8]. Deep saline aquifers, in particular, offer the largest global storage capacity and are therefore considered one of the most promising long-term storage options [9]. Although the engineering feasibility of CO_2 injection has been widely demonstrated, monitoring the long-term stability and geochemical evolution of the stored CO_2 remains a critical challenge. Solubility trapping involves the dissolution of CO_2 into formation brine, forming carbonic acid that dissociates into bicarbonate (HCO_{3^-}) and carbonate ($CO_{3^{2-}}$) ions [10]. These dissolved carbonate species alter the pore-fluid chemistry, ionic strength, and potential reservoir properties through dissolution–precipitation reactions [11], highlighting the importance of developing monitoring tools capable of detecting carbonate-rich fluids rather than focusing solely on free-phase CO_2.

The electrical resistivity method is a noninvasive geophysical approach for characterizing subsurface fluid distribution and has long been applied in hydrogeology and petroleum engineering[12]. In relatively clean carbonate systems, the bulk resistivity is largely controlled by the pore-fluid conductivity and porosity, as described by Archie's foundational relationship[12]. Therefore, variations in ionic composition and salinity directly influence the electrical response, suggesting that resistivity measurements may be sensitive to the dissolved carbonate species generated during CO_2 solubility trapping. Early investigations established the dependence of resistivity on saturation and salinity, which formed the basis for modern petrophysical interpretation[12]. More recent studies have extended these concepts to CCS monitoring, primarily focusing on detecting free-phase CO_2 plumes because of their high resistivity relative to that of formation brines[14]. Although effective for tracking plume migration, this approach is inherently less sensitive to dissolved carbonate ions, which are a key mechanism for long-term CO_2 storage.

Experimental studies have revealed that saturating carbonate rock samples with CO-saturated brines causes changes in the rock properties. Mineral dissolution experiments demonstrated that calcite-rich formations are highly reactive under CO_2 storage conditions, leading to measurable changes in porosity and permeability[8]. Additional work investigating acid-driven wormholing processes highlighted how fluid chemistry evolution influenced both the mechanical behavior and petrophysical properties of carbonate rocks[13]. Recent studies on rock properties under CO_2 storage conditions have suggested that salinity in CO_2-saturated brines affects wormhole formation and rock stiffness, thus showing the importance of monitoring dissolved carbonate species in addition to the supercritical CO_2 phase[15]. However, these studies have focused more on core flooding, geochemical modeling, and mechanical tests, whereas electrical geophysical tests have received limited attention.

Austin Chalk is a highly porous Upper Cretaceous formation commonly used as an analog for carbonate reservoirs because of its relatively simple mineralogy and consistent petrophysical characteristics. Micropetrographic and X-ray diffraction (XRD) analyses indicate that Austin Chalk is composed predominantly of calcite with minimal clay or dolomite content, thereby reducing surface conduction effects and allowing the fluid-controlled electrical behavior to be more clearly isolated[16]. Recent geoelectrical investigations of carbonated brine injection in carbonate aquifers have demonstrated the potential of electrical methods for monitoring CO_2 storage. However, the reported frequency dependence and electrode configuration responses are

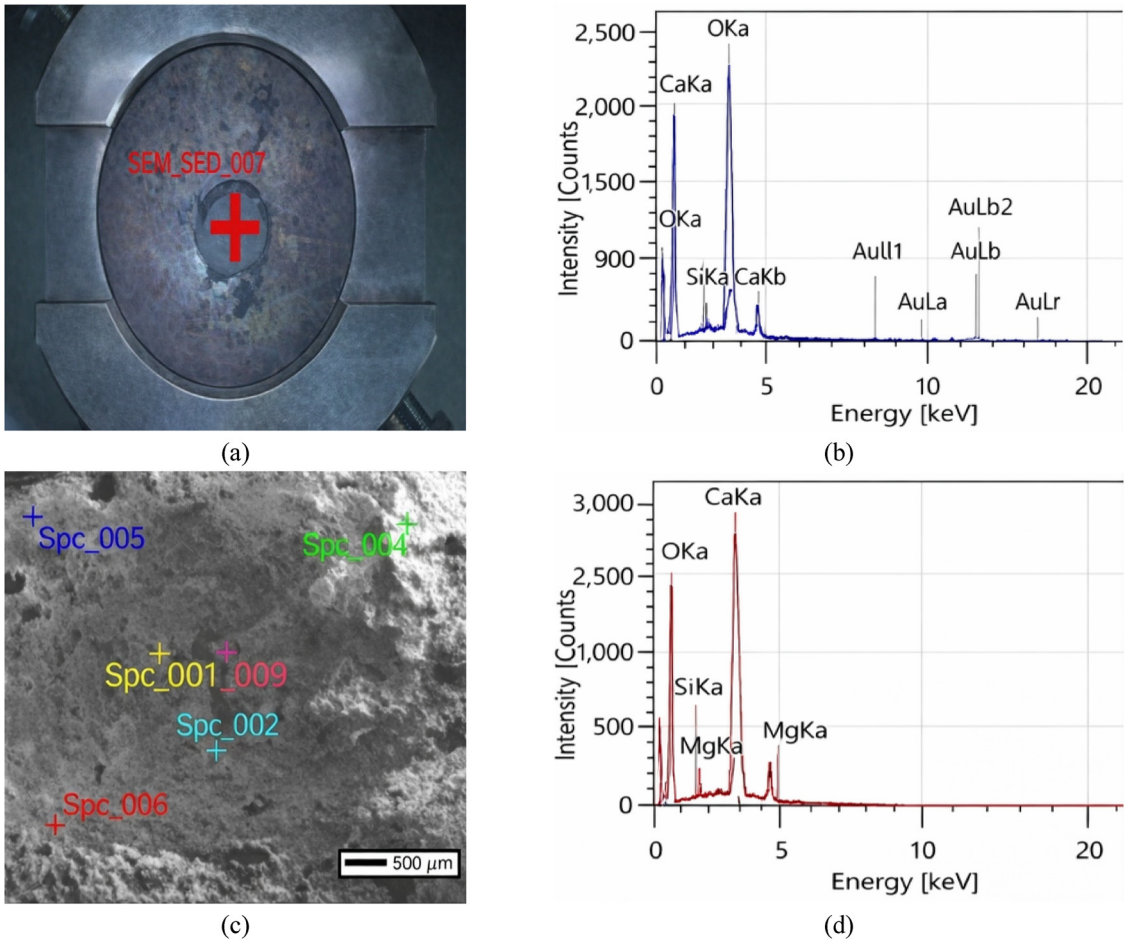

Figure 1. Scanning electron microscope (SEM) images and energy-dispersive X-ray spectroscopy (EDS) analyses of the Austin Chalk carbonate sample. (a) Core holder and SEM sampling location. (c) SEM micrograph showing analyzed spots. (b) and (d) Representative EDS spectra indicating the dominant elemental composition of the carbonate matrix. Modified after Helmi et al. (2025)[14]

Table 1. *Material and fluid properties*

Material	Description	Initial Porosity (%)
Austin Chalk	Limestone (>90% Calcite)	25–27
Formation Age	Upper Cretaceous	-
Permeability	8–15 mD	-
UCS	2500–3000 psi	-
Homogeneous	No	-
PW Base	High-salinity Brine	-
DI Base	Deionized Water	-
Additive	Potassium Carbonate (K_2CO_3) (0.1–5 wt%)	-

inconsistent across experimental setups[14]. These inconsistencies raise questions regarding the measurement precision and practical limits of resistivity monitoring in carbonate reservoirs.

Despite the extensive body of CCS research, only a limited number of studies have systematically evaluated whether electrical resistivity can be used to monitor carbonate-rich fluids quantitatively. Most existing studies rely on NaCl brines or live CO_2 systems, where the influences of the carbonate concentration, measurement frequency, and electrode configuration remain poorly constrained[14]. As a result, a clear knowledge gap exists regarding the detectability limits and reliability of electrical resistivity for monitoring solubility-trapping processes in carbonate formations such as Austin Chalk.

This study addresses that gap by evaluating the resistivity response to controlled carbonate concentrations using potassium carbonate (K_2CO_3) as a surrogate carbonate source. The use of K_2CO_3 allows precise control of dissolved carbonate levels under laboratory conditions, which is difficult to achieve using pure CO_2 because of phase behavior and solubility limitations. Experiments were conducted in deionized water (DI) and synthetic produced water (PW) over a concentration range of 0.1–5 wt%, with measurements at 12 Hz, 1 kHz, and 10 kHz. The investigation was extended to rock–fluid systems using Austin Chalk cores with well-characterized porosity and mineralogy to evaluate the influence of the rock matrix on bulk resistivity. By isolating the fluid chemistry effects from rock-controlled parameters, this study established a quantitative baseline for assessing the feasibility of electrical resistivity as a monitoring tool for carbonate-rich fluids associated with CO_2 solubility trapping.

2. METHODOLOGY

2.1. Materials and Brine Preparation. The brines used in this study were prepared using analytical-grade K_2CO_3 dissolved in both DI and PW. Austin Chalk limestone sister cores were selected as the rock samples for all rock–fluid interaction experiments and were cut to uniform dimensions (length: 2.8 inches, ~7.11 cm; diameter: 1.5 inches, ~3.8 cm) to ensure consistency across all measurement frequencies.

Two fluid systems were prepared to simulate different reservoir baselines:

1. DI: Used as a control to isolate the rock-fluid interaction.
2. Synthetic PW: Prepared to mimic the complex chemistry of deep-formation brines. The composition per liter of DI was: 53.668 g NaCl, 8.515 g $MgCl_2$ · 6H2O, 18.817 g $CaCl_2$ · $2H_2O$, and 1.351 g Na_2SO_4.

Analytical-grade potassium carbonate (K_2CO_3) was added to these base fluids at varying concentrations: 0.1, 0.25, 0.5, 0.75, 1, 2, 3, 4, and 5 wt%. The comprehensive physical and mineralogical properties of the materials and fluids, including the initial porosity and mechanical strength of the Austin Chalk, are summarized in Table 1.

Figure 1 shows the mineralogical composition and microtexture of the Austin Chalk limestone samples as determined by scanning electron microscopy–energy dispersive X-ray spectroscopy (SEM–EDS) characterization. As can be observed, the calcite-dominated carbonate matrix is accompanied by only minor accessory phases, confirming the relative mineralogical simplicity of the rock and minimizing the influence of clay-related surface conduction on the electrical measurements.

2.2. Test Workflow . Experiments were conducted using a custom hydrostatic core holder equipped with two to four electrode arrays for the rock–fluid system. This configuration minimizes contact resistance, which is critical for measuring conductive saline fluids. The experimental workflow is illustrated in Figure 2 , representing the sequential analysis of both the fluid system and the integrated rock–fluid system. The procedure involves four key stages:

1. Fluid characterization: Measurement of density, viscosity, pH, resistivity of bulk fluids, and temperature. Baseline resistivity measurements at frequencies of 12 Hz, 1 kHz, and 10 kHz with multi concentrations of K_2CO_3 solutions (DI or PW) were established for the fluid system to verify the electrical properties of the brine before core introduction.
2. Core saturation: Vacuum-saturation of dry sister limestone cores with K_2CO_3 solutions (DI or PW with multi concentrations).
3. Porosity analysis: The gravimetric porosity of each core was calculated by comparing the dry and wet weights, ensuring that the samples were fully saturated. 1
4. Resistivity measurement: The resistivity was measured at frequencies of 12 Hz, 1 kHz, and 10 kHz using two- and four-electrode systems.

Table 2. *Austin chalk core properties and calculated porosity*

Sample Environment	Concentration (wt%)	Dry Weight (g)	Wet Weight (g)	Porosity (%)
Austin Chalk + DI	0.1	180.66	201.20	25.37
Austin Chalk + DI	5.0	175.55	197.67	26.16
Austin Chalk + PW	0.1	175.75	198.50	26.45
Austin Chalk + PW	5.0	177.87	199.98	25.11

3. EXPERIMENTAL WORK

3.1. Fluid-only system. For the fluid-only system measurements, K_2CO_3 brines solutions were prepared in DI and PW under ambient temperature and pressure. Solutions with various concentrations (0.1, 0.25, 0.5, 0.75, 1, 2, 3, 4, and 5 wt%) were prepared to examine how the resistivity varied with increasing salt content. Prior to the readings, the temperature and pH of each solution were recorded. The resistivity was then measured using a benchtop dip-cell resistivity meter at three frequencies—12 Hz, 1 kHz, and 10 kHz—for DI.

3.1.1. Fluid + rock system. To evaluate the interaction between the K_2CO_3 brine solutions and Austin Chalk, cylindrical core samples were cut to approximately 2.8 inches in length and 1.5 inches in diameter. The end faces were leveled to ensure a proper fit within the benchtop resistivity setup. The dry weight of each sample was measured. The samples were then vacuumed according to their pore structures and saturated over four to five nights.

After saturation, the wet weight of each core was recorded and used to calculate the gravimetric porosity based on the dry and saturated masses. Resistivity measurements were then carried out using the two- and four-electrode configurations at 12 Hz, 1 kHz, and 10 kHz under the same conditions applied during the fluid-only phase. The physical properties and calculated porosities of the Austin Chalk cores are summarized in Table 2.

3.2. Instrumentation. All instruments were calibrated before testing to minimize measurement uncertainty and ensure repeatability across frequencies and fluid systems. In addition, all experiments were carried out on an integrated benchtop measurement platform designed to ensure accurate and repeatable characterization of the electrical and physicochemical properties in both fluid-only and rock–fluid systems, as shown in Figure 3 . Baseline resistivity measurements were first determined for the prepared brines using the benchtop dip-cell resistivity setup, as illustrated in Figure 3 (a), before introducing the rock samples to isolate the fluid-controlled electrical behavior. Core saturation was conducted in a vacuum chamber, as shown in Figure 3 (b), to ensure that the rock pore spaces were fully occupied with fluids and that the air content, which is known to introduce substantial uncertainty in the resistivity measurements of porous rock, was kept at a minimum. Bulk resistivity measurements were performed using a high-precision impedance analyzer, shown

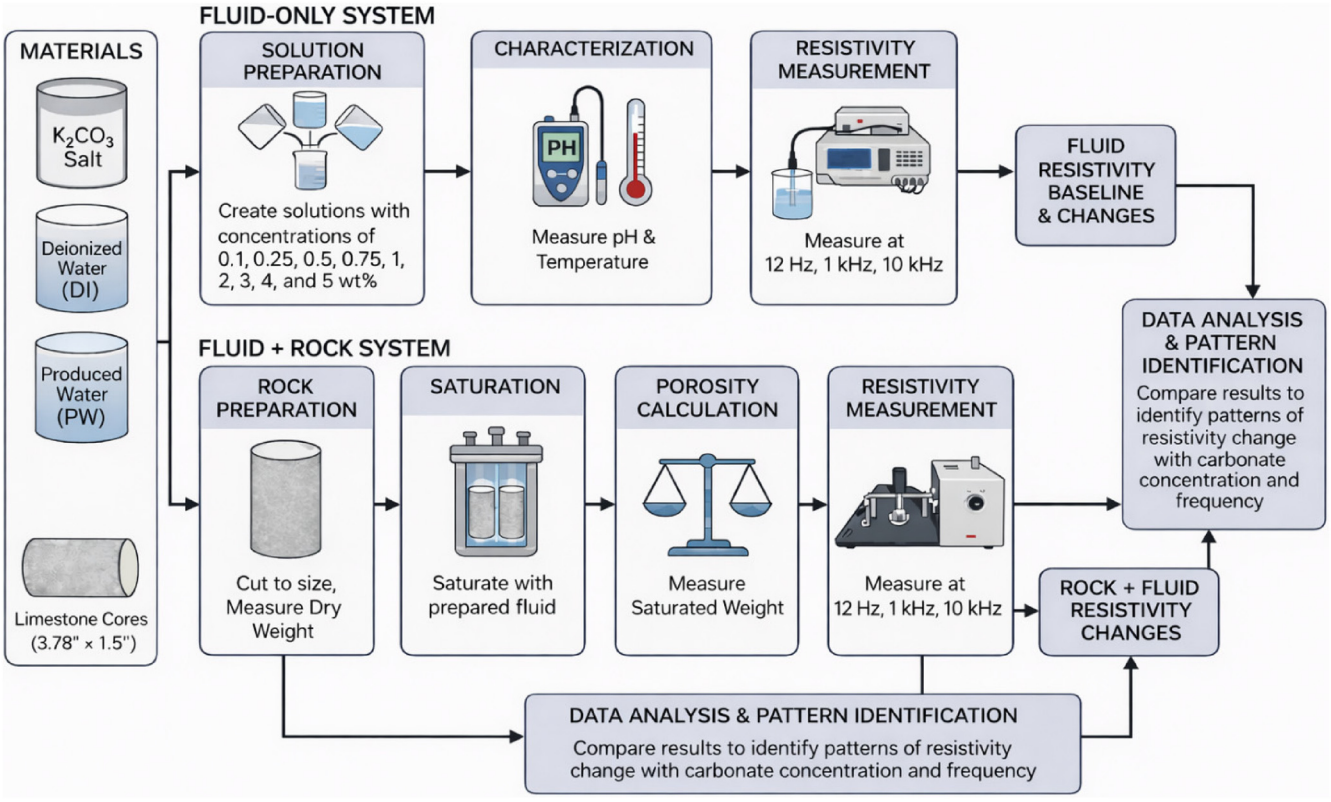

Figure 2. Workflow for detecting carbonate levels

in Figure 3 (c), which can be operated in both two- and four-electrode configurations. The precision of the impedance analyzer can be set at ±0.05%, covering a frequency range of 12 Hz to 200 kHz. This allowed for a systematic evaluation of the frequency-dependent effects and electrode configuration sensitivity. The four-electrode configuration was used to reduce electrode polarization and resistance, particularly in highly conductive brines, whereas the two-electrode configuration was used for a comparative assessment of the robustness of the measurements.

The fluid chemistry was continuously monitored using a benchtop electrochemical meter, as illustrated in Figure 3 (d), with the capability to measure pH, oxidation–reduction potential (ORP), and temperature with a resolution of ±0.01 pH units. This ensured that changes in electrical response could be understood in the context of well-controlled chemical conditions, especially considering the highly alkaline nature of the K_2CO_3 solutions. The densities and kinematic viscosities of the carbonate brines were measured using a calibrated viscometer, as shown in Figure 3 (e). This instrument measures density and kinematic viscosity simultaneously, and is useful in assessing changes in these properties with increasing concentrations of carbonate. Gravimetric measurements were performed using a semi-micro analytical balance, as shown in Figure 3 (f), with a resolution of 0.01 mg. This balance was used to accurately prepare the concentrations of K_2CO_3 and to measure the dry and saturated masses of the core used to calculate porosity. This instrumentation suite was used to control and measure the electrical, chemical, and physical properties, and to ensure that changes in resistivity could be attributed to changes in the frequency and concentration of the carbonate solutions rather than experimental uncertainty.

Figure 3. Experimental setup for carbonate brine characterization: (a) solution resistivity device; (b) vacuum saturation chamber for Austin Chalk cores; (c) GW Instek LCR 821 for resistivity measurements; (d) Hanna Instruments device for pH, redox potential, and temperature; (e) Anton Paar viscometer for viscosity and density; and (f) A&D GR semi-microbalance for solution preparation and porosity verification

Table 3. *Electrical and pH measurements of K_2CO_3 in deionized water*

Concentration	pH	Res_12 Hz	Res_1 kHz	Res_10 kHz
0.1	11.17	5.2711305	5.315967	5.315546
0.25	11.44	2.1985041	2.18080105	2.18088525
0.5	11.56	1.150287775	1.1748847	1.17533517
0.75	11.65	0.8058361	0.83961714	0.8414527
1	11.68	0.66918371	0.70668639	0.708364075
2	11.84	0.31378814	0.34663456	0.34716081
3	11.93	0.2632513	0.26571415	0.26664035
4	12	0.19581973	0.19784053	0.198865665
5	12	0.162865955	0.164343665	0.165194085

4. RESULTS AND DISCUSSION

The results of this study demonstrate the sensitivity of the ER method to varying carbonate concentrations and solvent types within Austin Chalk limestone. The following sections analyze the resistivity trends across fluid-only systems and saturated rock–fluid systems.

4.1. Fluid-only Resistivity Trends. The electrical resistivity of the K_2CO_3 solutions, both DI and PW, exhibited a significant, non-linear decrease as concentration increased from 0.1 to 5 wt%. This trend is fundamental for monitoring geochemical reactions and CO_2–brine–rock interactions in deep saline aquifers. As detailed in Table 3, the resistivity of the DI system at 1 kHz decreased rapidly from 5.316 Ω· m at 0.1 wt% to 0.164 Ω· m at 5 wt%, representing a substantial reduction of approximately 96.9%. This high-contrast geophysical signature, illustrated in Figure 4 , tracks the resistivity response across the tested concentration range. In addition, Figure 4 shows that the pure fluid resistivity values remained nearly identical across the tested frequency spectrum of 12–10 kHz.

By contrast, the PW system characterized in Table 4 and Figure 5 maintained a significantly lower baseline resistivity due to its inherent high salinity, with values decreasing from 0.087 Ω· m at 0.1 wt% to 0.066 Ω· m at 5 wt%. Although the relative change in the PW system was dampened compared to that in the DI system, both environments demonstrated a clear inverse relationship between the carbonate concentration and resistivity across the tested range. This comparison is highlighted in Figure 6 , which shows that the high ionic strength of the host brine acted as a conductive mask, reducing the relative signal of the added K_2CO_3. The physical properties of the PW solvent also showed measurable shifts, with the baseline density recorded at 0.1 wt% and a slight increase in viscosity from 1.13 to 1.15 cP, as depicted in the profiles in Figure 7 .

Furthermore, the pH measurements presented in Tables 3 and 4 reflect a marked increase in alkalinity with increasing carbonate enrichment. In the DI system, the pH rose from 11.17 to 12.0, whereas in the PW system, it increased from 8.02 to 10.83. As illustrated in Figure 8 , these pH shifts serve as critical secondary

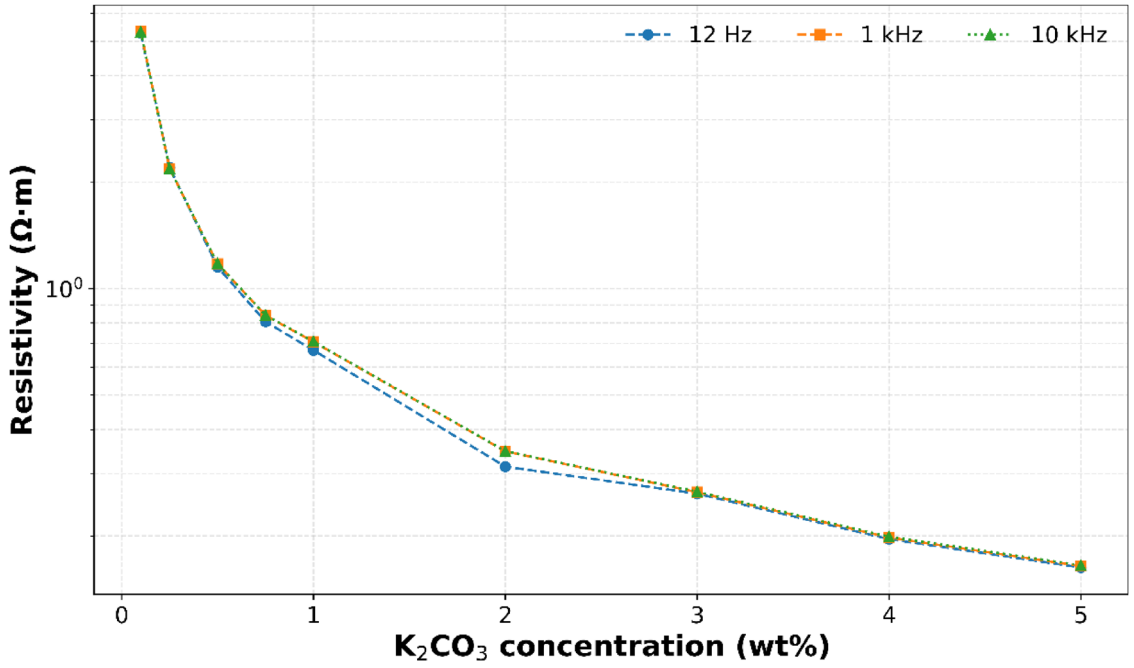

Figure 4. Electrical resistivity as a function of K_2CO_3 concentration in deionized water at different frequencies

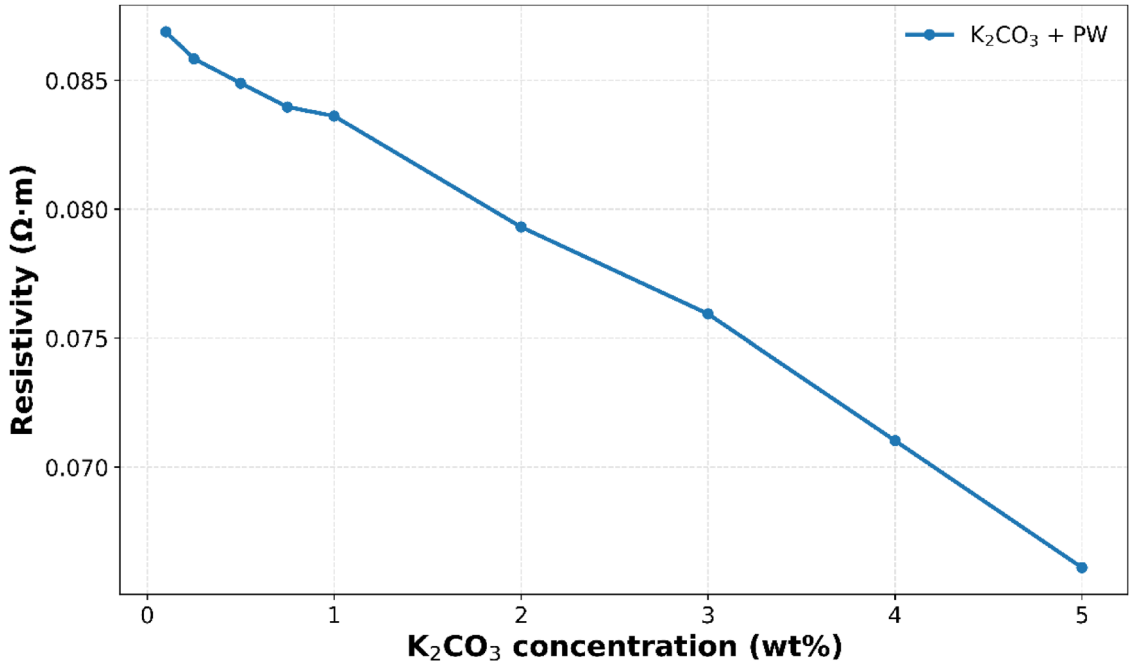

Figure 5. Electrical resistivity as a function of K_2CO_3 concentration in produced water

indicators for detecting geochemical equilibrium shifts during the carbon sequestration processes. The correlation between increasing pH and decreasing resistivity provides a robust framework for multiparameter reservoir monitoring.

4.2. Austin Chalk Saturated Core Results. The bulk resistivity in the Austin Chalk cores (porosity ~25%–27%) decreased in line with the fluid-only systems; however, the measured values were higher because the limestone matrix was resistive and reduced the pore volume available for the ionic current flow. A comparison of the 4-electrode measurements in Table 5 with the 2-electrode measurements in Table 6 shows that the 2-electrode setup reports a higher resistivity at every tested frequency for each brine type. For example, at 0.1 wt% K_2CO_3 in DI at 1 kHz, the 2-electrode configuration recorded 81.647 Ω· m (Table 6), whereas the 4-electrode setup recorded a significantly lower value, 65.921 Ω· m (Table 5). This discrepancy is attributed to the inclusion of the contact resistance and electrode polarization in the 2-electrode setup, whereas the 4-electrode configuration isolates the true bulk properties of the saturated rock.

The sensitivity of these electrical signatures to the carbonate levels is heavily influenced by the background fluid

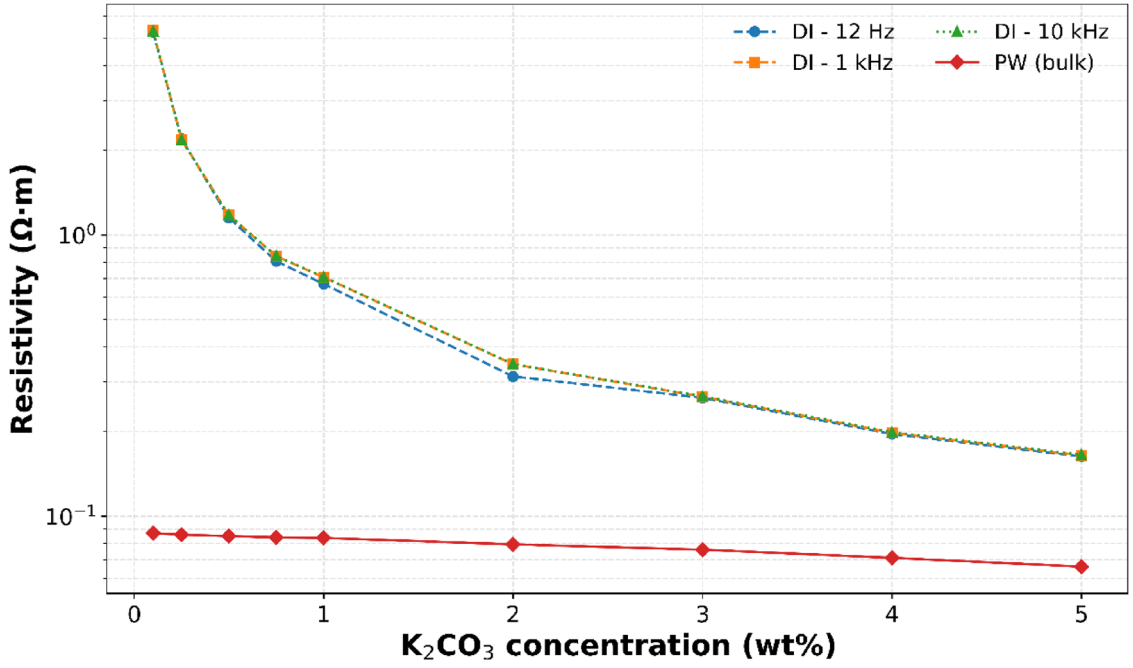

Figure 6. Comparison of electrical resistivity across varying K_2CO_3 concentrations for deionized water and produced water solvents

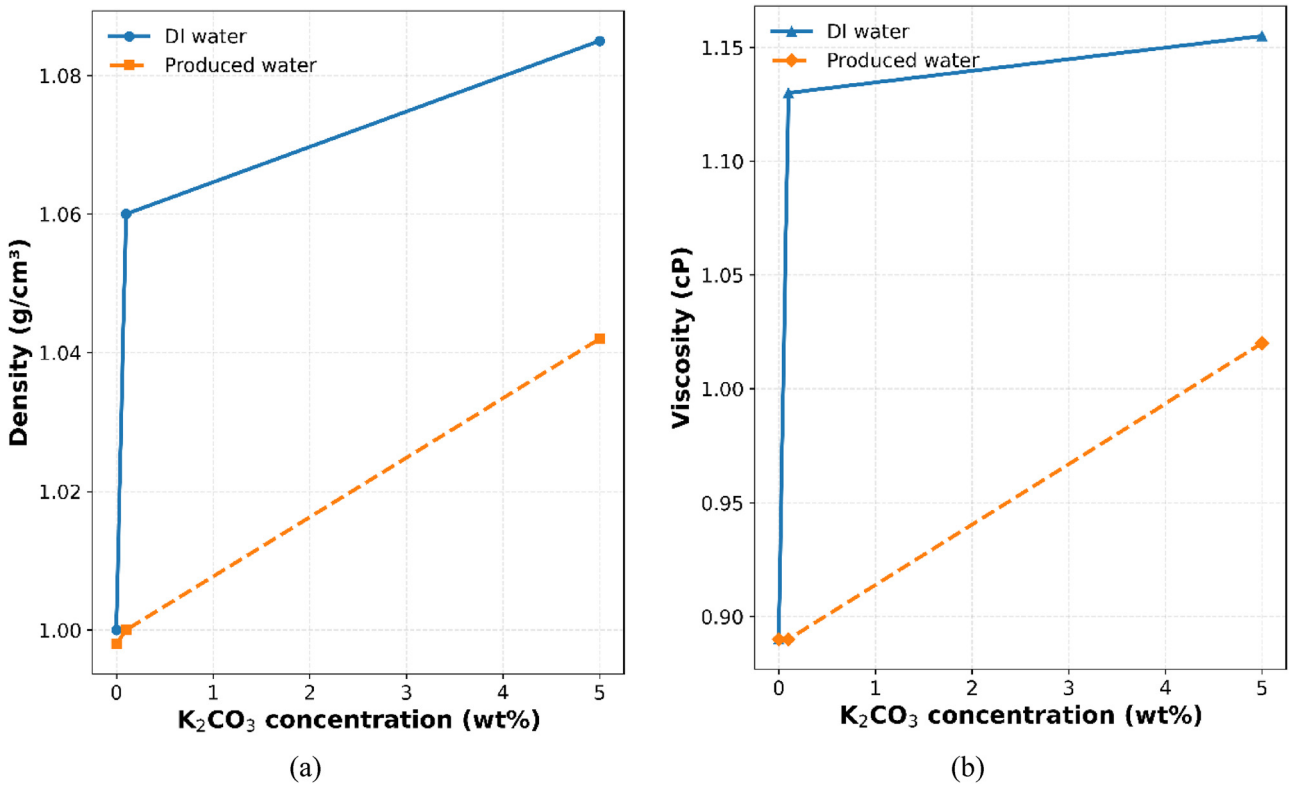

Figure 7. Variation of (a) density and (b) viscosity of deionized water and produced water with varying concentrations of K_2CO_3 (0.1 and 5 wt%)

environment. In the DI-saturated Austin Chalk, increasing the K_2CO_3 concentration led to a substantial resistivity drop from 65.921 to 1.072 Ω· m (at 1 kHz, 4e), indicating high diagnostic sensitivity in low-salinity aquifers. Conversely, as can be observed in Table 5, the PW environment demonstrated a much more attenuated response, with resistivity values only shifting from 1.815 to 1.496 Ω· m. This behavior confirms that the high initial ionic strength of PW acts as a conductive mask that dampens the relative impact of additional carbonate ions. Furthermore, the data in Table 5 highlights the frequency-dependent response or dispersion. At 0.1 wt% concentration, the bulk resistivity drastically declines from 80.605 Ω· m at 12 Hz to 66.040 Ω· m at

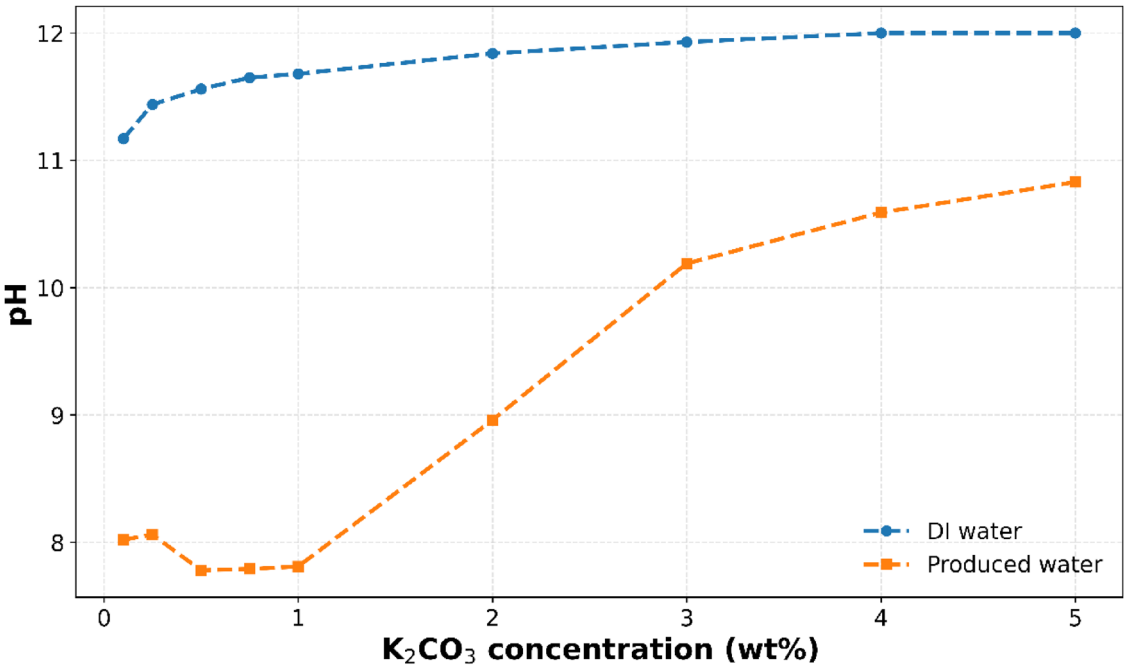

Figure 8. Variation of pH of deionized water and produced water with varying concentrations of K_2CO_3 (0.1 and 5 wt%)

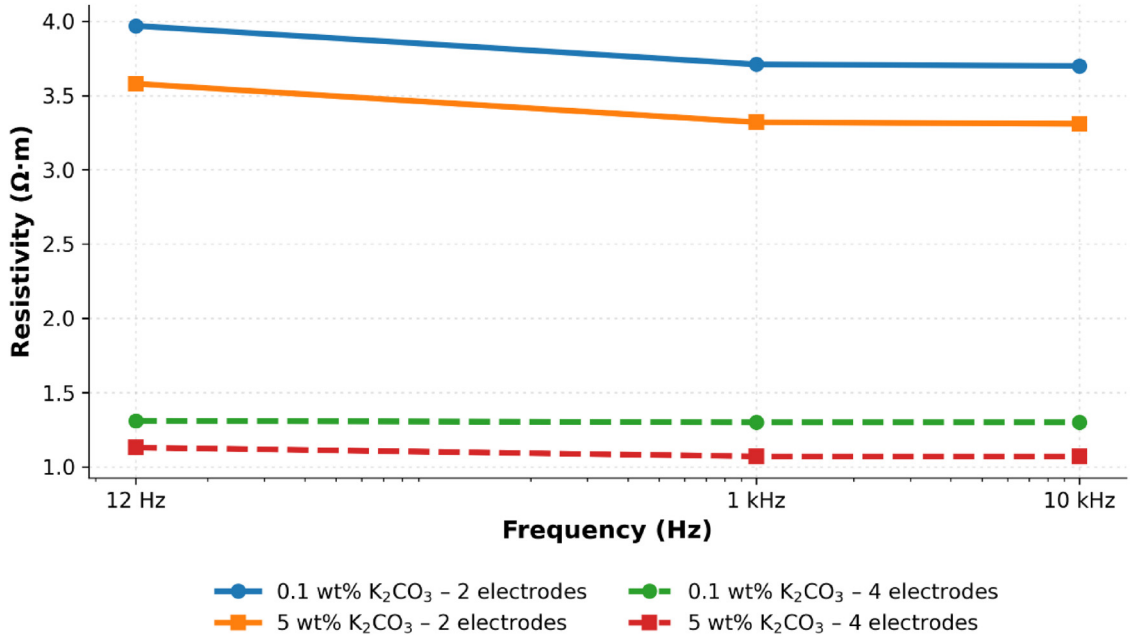

Figure 9. Comparative analysis of 2- and 4-electrode resistivity measurements for Austin Chalk samples across frequencies from 12 Hz to 10 kHz. The samples were saturated with DI containing 0.1 and 5 wt% K_2CO_3 to illustrate the discrepancy between measurement techniques at varying salinity levels

10 kHz. This sharp reduction indicates that at higher frequencies, the electrical signal is better able to bypass the polarization barriers at the rock–fluid interface and within the narrow pore throats of the limestone. In the PW-saturated system, the dispersion follows a similar pattern, dropping from 3.266 to 1.110 Ω· m at the same frequencies. Collectively, these results demonstrate that while electrical resistivity is a robust indicator of carbonate levels, the most accurate characterization is achieved using 4-electrode measurements and accounting for the frequency-dependent behavior of the specific host aquifer fluid.

The patterns shown in Figures 9 and 10 support the numerical differences observed between the 2- and 4-electrode methods. Figure 9 shows that in a low-salinity DI solution, the 2-electrode approach overestimates the resistivity at low frequencies because ions accumulate at the electrode–fluid interface and cause electrode polarization. However, the 4-electrode setup largely avoids this artifact by separating the electrodes used to drive the current from those used to measure the voltage. Figure 10 shows that the high ionic strength of PW lowers the bulk resistivity; however, a consistent difference remains between the two

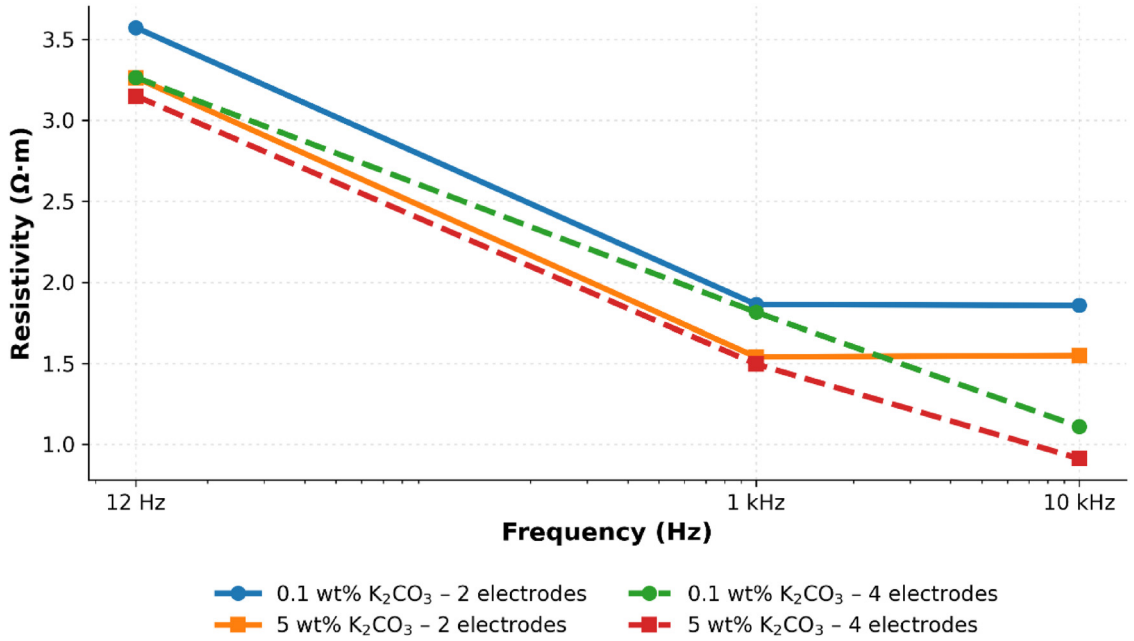

Figure 10. Comparative analysis of 2- and 4-electrode resistivity measurements for Austin Chalk samples across frequencies from 12 Hz to 10 kHz. The samples were saturated with produced water containing 0.1 and 5 wt% K_2CO_3 to illustrate the discrepancy between measurement techniques at varying salinity levels

Table 4. *Electrical and pH measurements of K_2CO_3 in produced water*

Concentration	pH	Res
0.1	8.02	0.086880973
0.25	8.06	0.08583691
0.5	7.78	0.084889643
0.75	7.79	0.083963056
1	7.81	0.08361204
2	8.96	0.079302141
3	10.19	0.075930144
4	10.59	0.071022727
5	10.83	0.066093853

measurement methods. This gap indicates that the contact resistance contributes meaningfully, even when the background brine salinity is high. Collectively, these results show that a 4-electrode setup is needed to measure the true frequency-dependent dispersion of the Austin Chalk because it reduces the artifacts that can mask carbonate concentration changes in a standard 2-electrode system.

4.3. Mechanistic Interpretation of Resistivity Behavior. The observed non-linear decrease in resistivity with increasing K_2CO_3 concentration reflects enhanced ionic conductivity within the pore fluid. This behavior is consistent with the fundamental relationship between the fluid conductivity and resistivity in porous media established by Archie's law[12]. Furthermore, the observed resistivity reduction aligns with recent geoelectrical evaluations of CO_2 storage, which demonstrate that increased ionic strength from carbonate species significantly enhances bulk conductivity[14]. This sensitivity is further influenced by the salinity of the host brine, because high-salinity environments can act as a conductive mask that dampens the electrical signature of the added carbonate species, a phenomenon observed in recent studies on CO_2–brine–rock interactions[15]. At low concentrations, the increase in carbonate ion availability significantly improves the charge transport pathways, resulting in rapid resistivity reduction. However, above approximately 3 wt%, the resistivity trend becomes relatively stable, suggesting that the conductive pathways approach saturation, and additional ions contribute less effectively to bulk electrical transport. The limited frequency dependence observed in the fluid-only systems indicates that conduction is dominated by ionic mobility rather than by interfacial polarization effects within the tested frequency range. In rock–fluid systems, the Austin Chalk matrix introduces tortuosity and geometric constraints that increase bulk resistivity while preserving the inverse relationship between carbonate concentration and electrical response.

4.4. Challenges and Scaling of CO_2 Monitoring Experiments. Pure CO_2 was not used in the current study because of the complexities involved in maintaining a stable dissolved CO_2 concentration. In its place, potassium carbonate, K_2CO_3, was employed owing to its stable chemical properties, which could simulate the effects of the carbonate-rich aqueous solution in a subsurface reservoir. The solubility of K_2CO_3 in water produces carbonate ions, which influence the ionic conductivity in the same manner as the dissolved CO_2, that is, HCO_{3-} and CO_{3-}. However, in a real subsurface reservoir, the dissolved CO_2 causes geochemical reactions, including reduction of pH, dissolution of minerals, and precipitation, which also influence the electrical properties. The current study showed the strong influence of carbonate concentration on the electrical properties. In future studies, CO_2 injection experiments will be performed to assess the applicability of the proposed method for CCS monitoring in real reservoir conditions.

5. CONCLUSIONS

This study demonstrated that ER can detect controlled K_2CO_3 concentration changes in both fluid-only and carbonate rock systems, thus providing a potential monitoring pathway for solubility-trapped CO_2. The main conclusions are as follows:

- The test specimens showed uniform electrical properties, validating the experimental setup.
- The solvent used significantly affects the resistivity, with DI leading to larger changes than the high-salinity PW.
- Electrode configuration is important; four-electrode setups better capture the true bulk resistivity.
- Frequency influences rock–fluid systems due to interfacial polarization. For example, the resistivity of DI-saturated Austin Chalk (0.1 wt%) dropped from 80.6 Ω· m at 12 Hz to 66.0 Ω· m at 10 kHz, whereas fluid-only systems remain frequency-independent.

Table 5. *Bulk resistivity of Austin Chalk cores (4-electrode system)*

Sample Environment	Concentration (wt%)	At 12 Hz (4e) Ω· m	At 1 kHz (4e) Ω· m	At 10 kHz (4e) Ω· m
Austin Chalk + DI	0.1	80.605	65.921	66.040
Austin Chalk + DI	5.0	1.126	1.072	1.074
Austin Chalk + PW	0.1	3.266	1.815	1.110
Austin Chalk + PW	5.0	3.151	1.496	0.913

Table 6. *Bulk resistivity of Austin Chalk cores (2-electrode system)*

Sample Environment	Concentration (wt%)	At 12 Hz (2e) Ω· m	At 1 kHz (2e) Ω· m	At 10 kHz (2e) Ω· m
Austin Chalk + DI	0.1	83.249	81.647	80.884
Austin Chalk + DI	5.0	3.584	3.318	3.310
Austin Chalk + PW	0.1	3.573	1.863	1.857
Austin Chalk + PW	5.0	3.264	1.540	1.549

- ER is highly sensitive at low K_2CO_3 concentrations (<3 wt%) but stabilizes at higher concentrations.

This study adds evidence to the research aimed at strengthening monitoring methods for carbon sequestration and describing the geochemical properties of subsurface reservoirs. Future research should focus on long-term studies of geochemical durability, dynamic flow conditions, and true CO_2–brine systems to evaluate field-scale geophysical tests and computational modeling. These steps will help extend the results to other settings and refine real-time monitoring approaches for high-salinity aquifers.

AFFILIATIONS AND AUTHOR DETAILS

Undergraduate Author

Abdullah Deya Al-Qisoom – *Department of Geosciences, King Fahd University of Petroleum & Minerals, Dhahran 31261, Saudi Arabia*; 0009-0000-6340-4879
Email: s202156590@kfupm.edu.sa

Corresponding Author

Ahmed Al-Yaseri – *Senior Research Scientist, Center for Integrated Petroleum Research, King Fahd University of Petroleum & Minerals, Dhahran 31261, Saudi Arabia*; 0000-0001-9094-1258
Email: ahmed.yaseri@kfupm.edu.sa

ACKNOWLEDGEMENTS

We also thank Ms. Maryam Sani Maigana for her assistance throughout this study. We are grateful to the Center for Integrative Petroleum Research for providing the facilities that enabled this study. We appreciate the support provided by Mr. Hisham Alqassab and the Undergraduate Research Office.

REFERENCES

(1) Davis, W. The relationship between atmospheric carbon dioxide concentration and global temperature for the last 425 million years. *Climate* 5, 76 (2017).

(2) Ajayi, T., Gomes, J. S. & Bera, A. A review of CO_2 storage in geological formations emphasizing modeling, monitoring and capacity estimation approaches. *Petrol. Sci.* **16**, 1028–1063 (2019).

(3) Allen, M. R. et al. A solution to the misrepresentations of CO_2-equivalent emissions of short-lived climate pollutants under ambitious mitigation. *npj Clim. Atmos. Sci.* **1**, 16 (2018).

(4) IPCC. Climate change 2021: The physical science basis. Contribution of Working Group I to the Sixth Assessment Report of the Intergovernmental Panel on Climate Change (*Cambridge Univ. Press, 2021*).

(5) Rosenbauer, R. J., Thomas, B., Bischoff, J. L. & Palandri, J. Carbon sequestration via reaction with basaltic rocks: Geochemical modeling and experimental results. *Geochim. Cosmochim. Acta* **89**, 116–133 (2012).

(6) Anika, O. C. *et al.* Prospects of low and zero-carbon renewable fuels in 1.5-degree net zero emission actualisation by 2050: A critical review. *Carbon Capture Sci. Technol.* **5**, 100072 (2022).

(7) Mwenketishi, G. T., Benkreira, H. & Rahmanian, N. A comprehensive review on carbon dioxide sequestration methods. *Energies* **16**, 7971 (2023).

(8) Black, J. R., Carroll, S. A. & Haese, R. R. Rates of mineral dissolution under CO_2 storage conditions. *Chem. Geol.* **399**, 134–144 (2015).

(9) Fatah, A. *et al.* Geochemical reactions of high total organic carbon oil shale during CO_2 treatment relevant to subsurface carbon storage. *Energy Fuels* **38**, 1161–1172 (2023).

(10) Romanov, V. *et al.* Mineralization of carbon dioxide: A literature review. *ChemBioEng Rev.* **2**, 231–256 (2015).

(11) Portier, S. & Rochelle, C. Modelling CO_2 solubility in pure water and NaCl-type waters from 0 to 300 °C and from 1 to 300 bar. *Chem. Geol.* **217**, 187–199 (2005).

(12) Archie, G. E. The electrical resistivity log as an aid in determining some reservoir characteristics. *Trans. AIME* **146**, 54–62 (1942).

(13) Mustafa, A. *et al.* Impact of acid wormhole on the mechanical properties of chalk, limestone, and dolomite: Experimental and modeling studies. *Energy Rep.* **8**, 605–616 (2022).

(14) Helmi, M. E. *et al.* Geoelectrical evaluation of CO_2 storage in carbonate aquifers using carbonated water injection. *Energy & Fuels* **39**, 18969–18979 (2025).

(15) Al-Dhafeeri, A. *et al.* The impact of CO_2 saturated brine salinity on wormhole generation and rock geomechanical and petrophysical properties. *Geoenergy Sci. Eng.* **233**, 212490 (2024).

(16) Loucks, R. G. *et al.* Micropetrographic characterization of a siliciclastic-rich chalk; Upper Cretaceous Austin Chalk Group along the onshore northern Gulf of Mexico, USA. *Sediment. Geol.* **412**, 105821 (2021).